Effect of Phase Transformation from h-BN to c-BN on Nanoparticle Fracture Tendency in AA8090/h-BN Particle-Reinforced Metal Matrix Composites

A. Chennakesava Reddy

Professor, Department of Mechanical Engineering, JNTU College of Engineering, Hyderabad, India
dr_acreddy@yahoo.com

Abstract: *In the present work, the AA8090-BNmetal matrix composites were manufactured at 10% and 30% volume fractions of BN. The composites were subjected to mechanical and thermal loads. The microstructure of AA8090 alloy-BN reveals the fracture of interphase and particle. The particle fracture was initiated with the phase transformation from h-BN to w-BN at 250^{o}C and from w-BN to c-BN at 300^{o}C due to combined thermal and tensile loading.*

Keywords: *AA8090, boron nitride, phase transformation, RVE model, finite element analysis, interphase fracture.*

1. INTRODUCTION

Unlike conventional materials, the properties of the composite material can be designed considering the structural aspects. The design of a structural component using composites involves both material and structural design. Composite properties (e.g. stiffness, thermal expansion etc.) can be varied continuously over a broad range of values under the control of the designer. In the past, various research works have been carried out on metal matrix composites prepared from aluminum alloy matrices and reinforced particles such as SiC [1-7], Al_2O_3 [8-12], TiO_2 [13-15], ZrO_2 [16], TiN [17], B_4C [18] ZrC [19], $Al(OH)_3$ [20] and graphite [21-22]. The stress transfer characteristic of nanoparticle reinforced composite materials under various mechanical and thermal loadings is very important for optimum utilization of metal matrix composites. The characteristics of low density and low thermal expansion of ceramics assume a great deal of importance in most applications. Boron nitride (BN) is a heat- and chemically resistant refractory compound of boron and nitrogen. It exists in various crystalline forms that are isoelectronic to a similarly structured carbon lattice. The hexagonal form (figure 1) corresponding to graphite is the most stable and soft among BN polymorphs, and is therefore used as a lubricant and an additive to cosmetic products. The cubic (sphalerite structure) variety analogous to diamond is called c-BN; it is softer than diamond, but its thermal and chemical stability is superior. The rare wurtzite BN modification is similar tolonsdaleite and may even be harder than the cubic form. Under combined loading of thermal and tension, the phase transformation is very important the optimum utilization BN particle based composites. According data presented in [23], shear deformations exert a considerable effect on phase transformations.

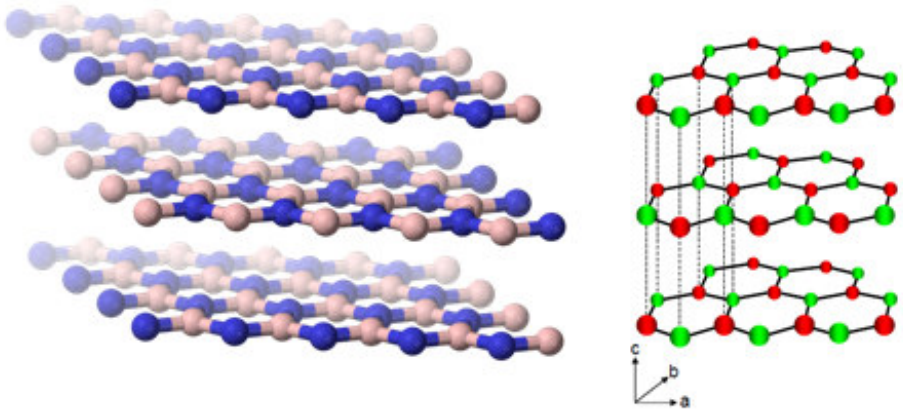

Figure 1: Hexagonal structure of BN.

Under combined loading of thermal and tension, the phase transformation is very important the optimum utilization BN particle based composites. In h-BN the atoms within the basal planes are bonded to three nearest neighbors through strong in-plane sp2 -hybridization, but the hexagonal planes are bonded to each other through weak van der Waals interaction only. This

bonding anisotropy leads to different physical properties depending on the crystal direction. In c-BN and w-BN, on the other hand, the atoms are bonded to four nearest neighbors of the alternating species through sp3 -hybridization. This results in a very short bond length leads to a high mass density and hardness that are comparable to those of diamond. A transition from h-BN to w-BN and r-BN to c-BN, respectively, involves two deformation processes: a lattice compression along the c axis and splitting of flat basal layers [24]. These changes result in an increase of density from 2.2 up to 3.5 g/cm3 and in a formation of sp3 hybridized tetrahedral bonds [25]. On the other hand, a direct transition from h-BN to c-BN and from r-BN to w-BN is unlikely, since it would require both breaking and changing the nature of chemical bonds [26]. Thus, the direct transformation from h-BN to c-BN requires the simultaneous application of very high temperatures and pressures in order to overcome the activation barrier for the conversion.

Finite element method (FEM) is capable of identifying the local response of the material. A common practice to estimate the bulk and local responses of composite material is to use a unit cell reinforced by a single fiber, whisker or particle subjected to periodic and symmetric boundary conditions [23]. A lot of research was carried out to assess the interface behavior in particle reinforced metal matrix composites under tensile loading using finite element analysis approach [14-20].

In the present work, hexagonal boron nitride (h-BN) was used to fabricate AA8090/h-BN composites. The effect of thermo-tensile loading on the fracture in AA8090 alloy/h-BN composites was examined. Both microscopic and micromechanics methods were employed to assess fracture in the composites. ANSYS software was used to computationally simulate thermo-mechanical nonlinear behavior of AA8090 alloy/BN composites to analyze local constituent response including the interface/interphase regions. The results obtained from the numerical simulation were validated with the experimental results.

2. MATERIALS METHODS

The matrix material was AA8090 alloy. The reinforcement material was BN nanoparticles of average size 100nm. AA8090 alloy/ BN composites were fabricated by the stir casting process and low pressure casting technique with argon gas at 3.0 bar. The composite samples were give solution treatment and cold rolled to the predefined size of tensile specimens. The heat-treated samples were machined to get rectangular specimens (figure 2) for the tensile tests. The tensile specimens were placed in the grips of a Universal Test Machine (UTM) with temperature controlled chamber at a specified grip separation and pulled until failure. The test speed was 2 mm/min. A strain gauge was used to determine elongation. In the current work, a cubical representative volume element (RVE) was implemented to analyze the tensile behavior AA8090/BN nanoparticle composites at two (10% and 30%) volume fractions of BN and at different temperatures. The shape BN nanoparticle considered in this work is spherical. The periodic particle distribution was a square array and corresponding representative volume element (RVE) as shown in figure 3. The large strain PLANE183 element was used in the matrix in all the models. In order to model the adhesion between the matrix and the particle, a CONTACT 172 element was used.

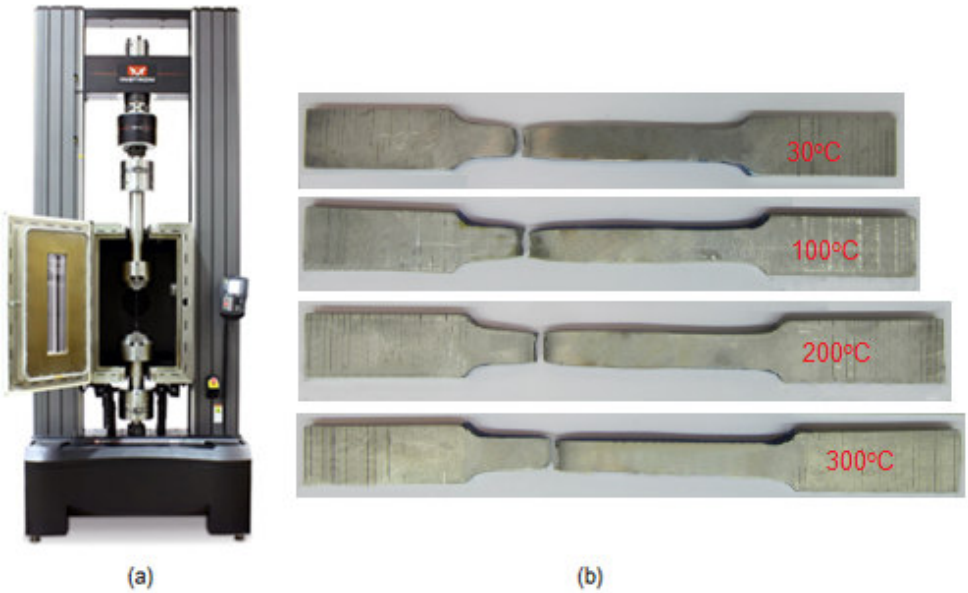

Figure 2: Tensile testing: UTM with temperature controlled chamber and (b) tested tensile specimens.

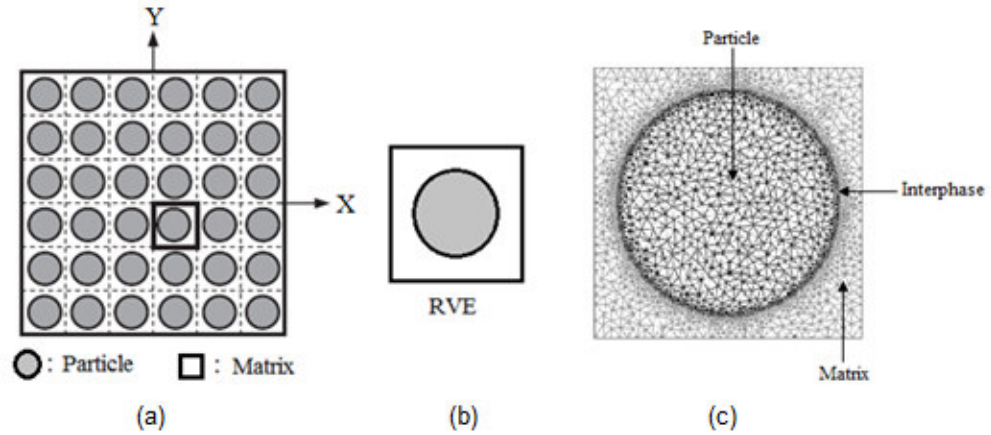

Figure 3: Square array of particles (a), Representative Volume Element (b) and Discretization of RVE (c).

The phase a transformation of BN was determined by Fourier transform infrared spectroscopy (FTIR) as shown in figure 4. The result of Fourier transformation is a spectrum of the signal at a series of discrete wavelengths.

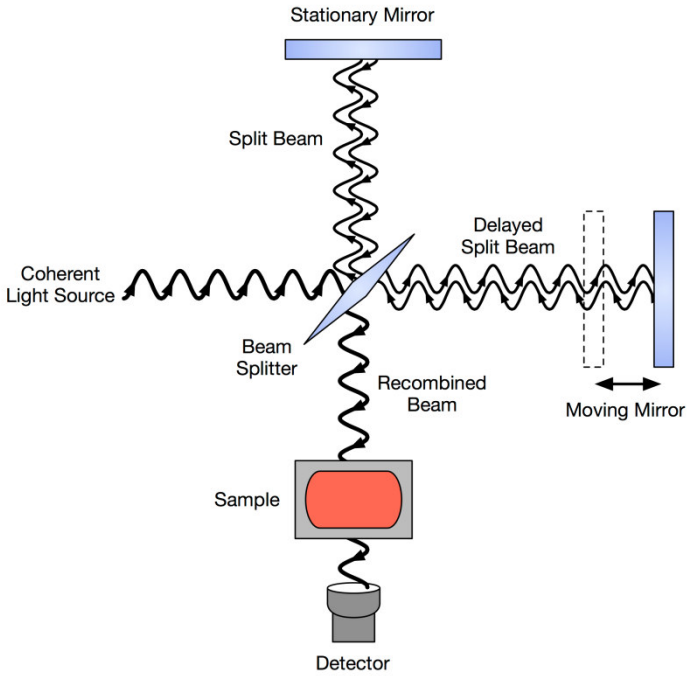

Figure 4: Fourier transform infrared spectroscopy.

3. RESULTS AND DISCUSSION

Boron nitride used in the present work was produced synthetically. Hexagonal boron nitride was obtained by the reacting boron trioxide (B_2O_3) or boric acid ($B(OH)_3$) with ammonia (NH_3) or urea($CO(NH_2)_2$) in a nitrogen atmosphere:

$$B_2O_3 + 2\ NH_3 \rightarrow 2\ BN + 3\ H_2O\ (T = 900\ °C)$$

$$B(OH)_3 + NH_3 \rightarrow BN + 3\ H_2O\ (T = 900\ °C)$$

$$B_2O_3 + CO(NH_2)_2 \rightarrow 2\ BN + CO_2 + 2\ H_2O\ (T > 1000\ °C)$$

$$B_2O_3 + 3\ CaB_6 + 10\ N_2 \rightarrow 20\ BN + 3\ CaO\ (T > 1500\ °C)$$

The resulting disordered (amorphous) boron nitride contains 92–95% BN and 5–8% B_2O_3. The remaining B_2O_3 can be evaporated in a second step at temperatures> 1500 °C in order to achieve BN concentration >98%. Such annealing also crystallizes

BN, the size of the crystallites increasing with the annealing temperature. The distribution of nanoparticles in a count of 30 is shown in figure 5 for the fabrication of AA8090/BN composites.

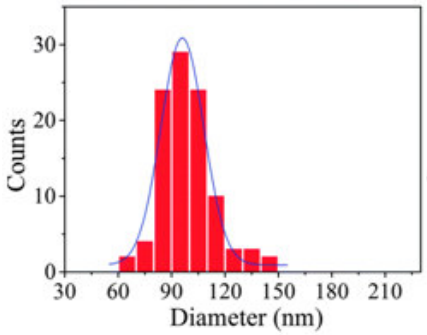

Figure 5: Particle distribution of BN.

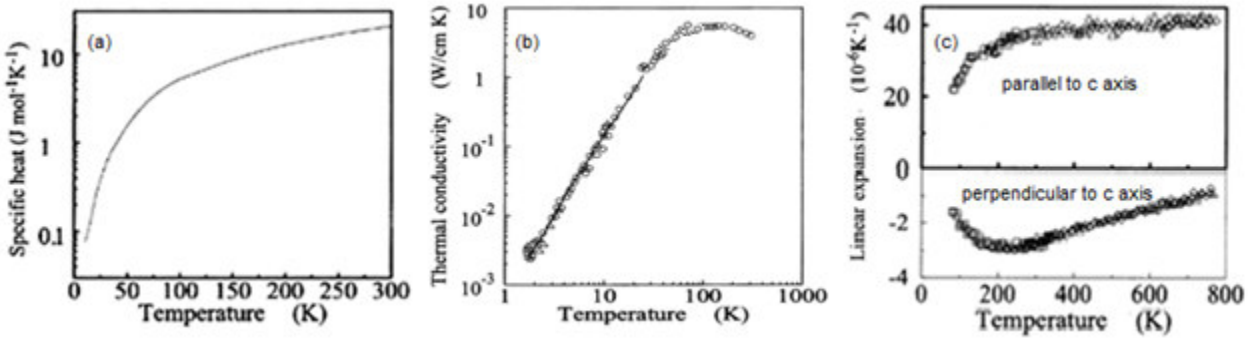

Figure 6: Thermal properties of BN.

The basic thermal properties required for the present work are shown in figure 6. Specific heat, thermal conductivity and coefficient of linear expansion were increased with temperature.

3.1 Thermo-Mechanical Behavior

Figure 7 represents micromechanical properties of AA8090/BN composites. The elastic modulus is normalized with the elastic modulus of AA8090 alloy. The normalized stiffness of the composites decreases with increase of temperature. The stiffness of AA8090 alloy/30% BN composites is higher than that of AA8090 alloy/10% BN composites (figure 7a). The normalized stiffness along the normal direction is lower than that along the load direction. There is discrepancy of stiffness along normal to load direction at 100°C. The reason is unknown. The normalized shear modulus is constant with increase of temperature for AA8090 alloy/BN composites (figure 7b). The major Poisson's ratio decreases initially from room temperature to 100°C and later on it increases with temperature (figure 7c).

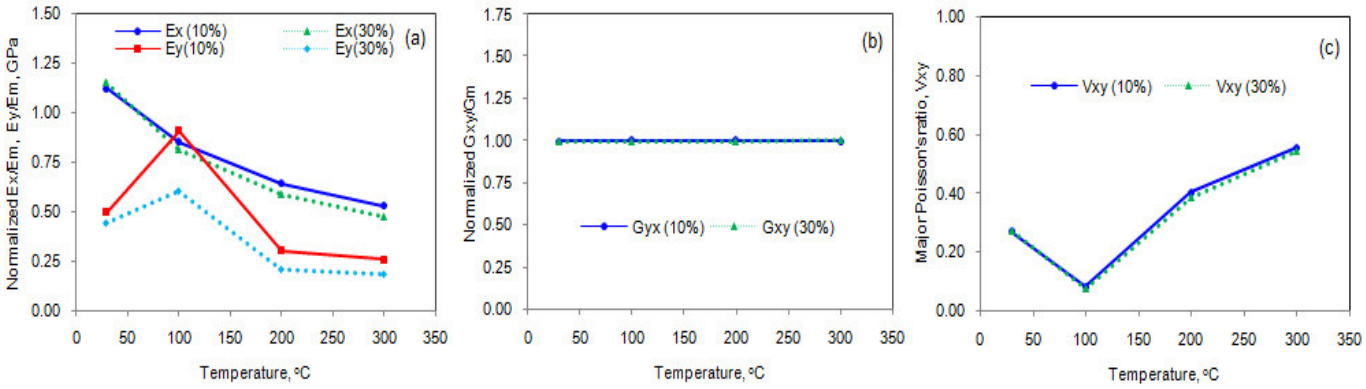

Figure 7: Effect of temperature on micromechanical properties of AA8090/BN composites.

3.2 Fracture Analysis

If the particle deforms in an elastic manner (according to Hooke's law) then,

$$\tau = \frac{n}{2}\sigma_p \quad (1)$$

where σ_p is the particle stress. If particle fracture occurs when the stress in the particle reaches its ultimate tensile strength, $\sigma_{p,uts}$, then setting the boundary condition at

$$\sigma_p = \sigma_{p,\,uts} \quad (2)$$

The relationship between the strength of the particle and the interfacial shear stress is such that if

$$\sigma_{P,uts} < \frac{2\tau}{n} \quad (3)$$

Then the particle will fracture. From the figure 8a, it is observed that the BN nanoparticle was fractured as the condition in Eq. (3) is satisfied above 100°C for the composites AA8090/BN. This is due to CTE and stiffness mismatches between BN nano-particles and AA8090 alloy matrix. For the interfacial debonding/yielding to occur, the interfacial shear stress reaches its shear strength:

$$\tau = \tau_{max} \quad (4)$$

For particle/matrix interfacial debonding can occur if the following condition is satisfied:

$$\tau_{max} < \frac{n\sigma_p}{2} \quad (5)$$

It is observed from figure 8b that the interphase debonding occurs between BN nanoparticle and AA8090 alloy matrix as the condition in Eq.(5) is satisfied at all temperatures for the composites AA8090/BN composites. The debonding phenomenon is high in the composites comprising of 10% BN.

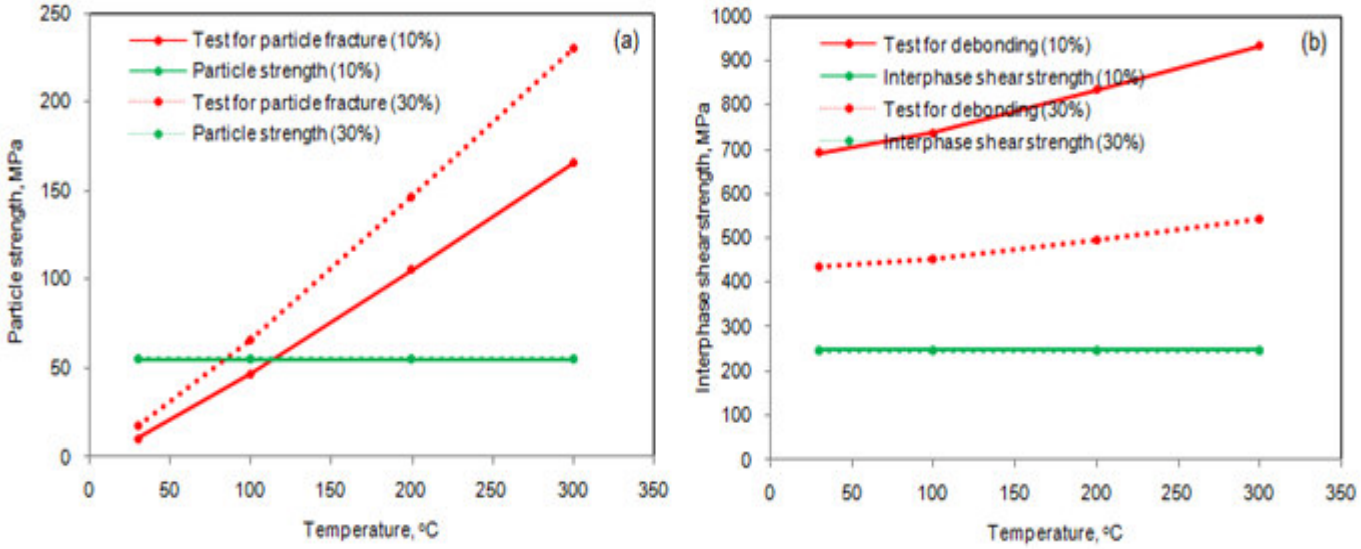

Figure 8: Criterion for interfacial for (a) particle fracture and (b) debonding.

The von Mises stress induced at the interface are higher than that induced in the nanoparticle (figure 9). Hence, the interfacial interphase fracture was occurred between the particle and the matrix. The particle fracture was occurred in all the composites as the von Mises stress exceeds the ultimate tensile strength of BN nanoparticles due to thermal shock. The microstructure shown in figure 10 confirms the occurrence of debonding (letter 'B') and particle fractures (letter 'A') in the composites. The microstructure also reveals the porosity (letter 'C') and clustering of particles.

According FTIR spectra (figure 11) it was found that hexagonal boron nitride (h-BN) began to transform into wurtzite boron nitride (w-BN) and cubic boron nitride (c-BN) at 220 °C. More and more h-BN converted into w-BN and c-BN with the in-crease in temperature, and this transformation process completed at 300 °C. The facture of BN nanoparticle in AA8090/BN composites is because of phase transformation from h-BN to w-BN and then c-BN (figure 12) when subjected to combined loading of temperature and tension.

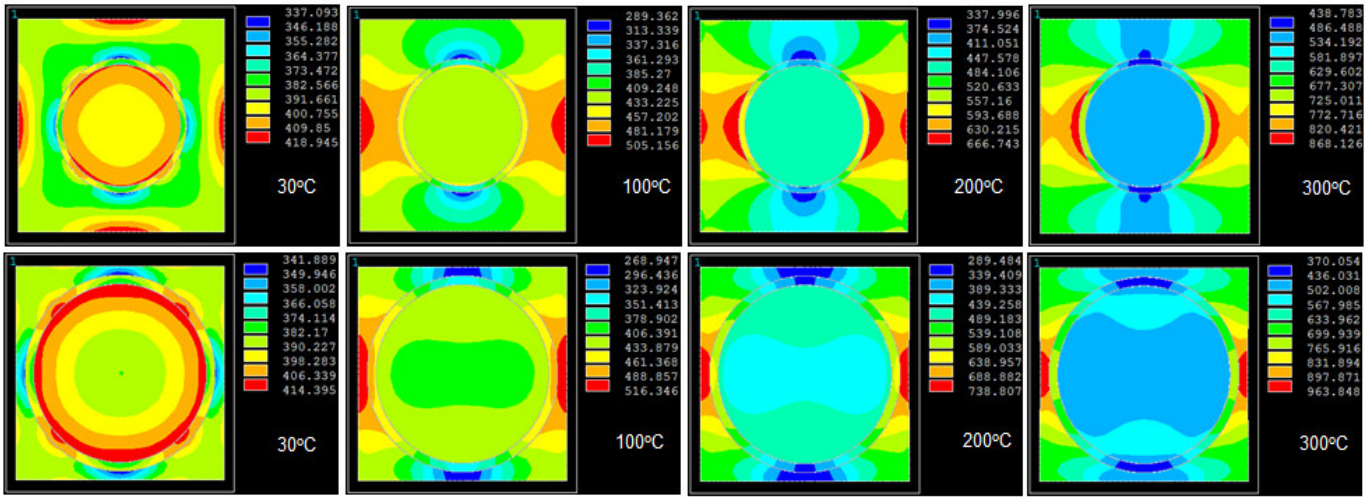

Figure 9: Images of von Mises stresses obtained from FEA: (a) AA8090/10% BN and (b) AA8090/30% BN composites.

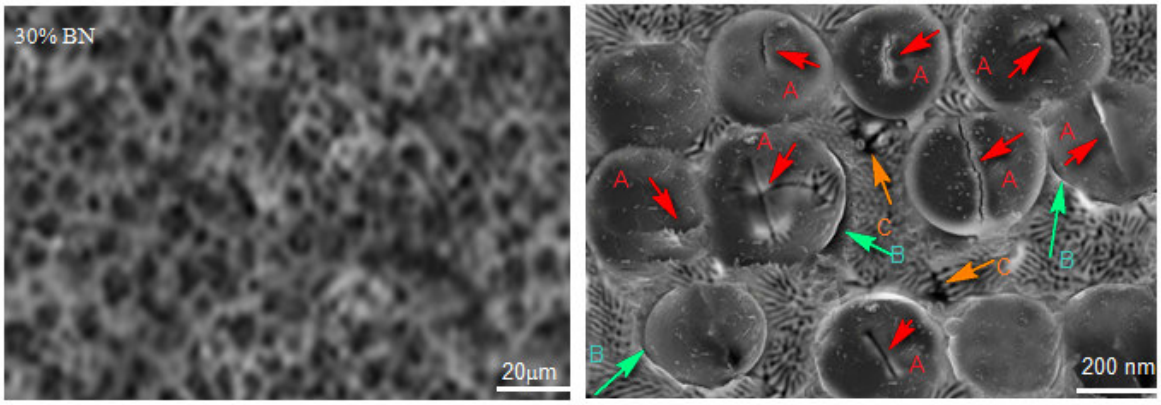

Figure 10: SEM image illustrating debonding and particle fracture in AA8090/30%BN composite.

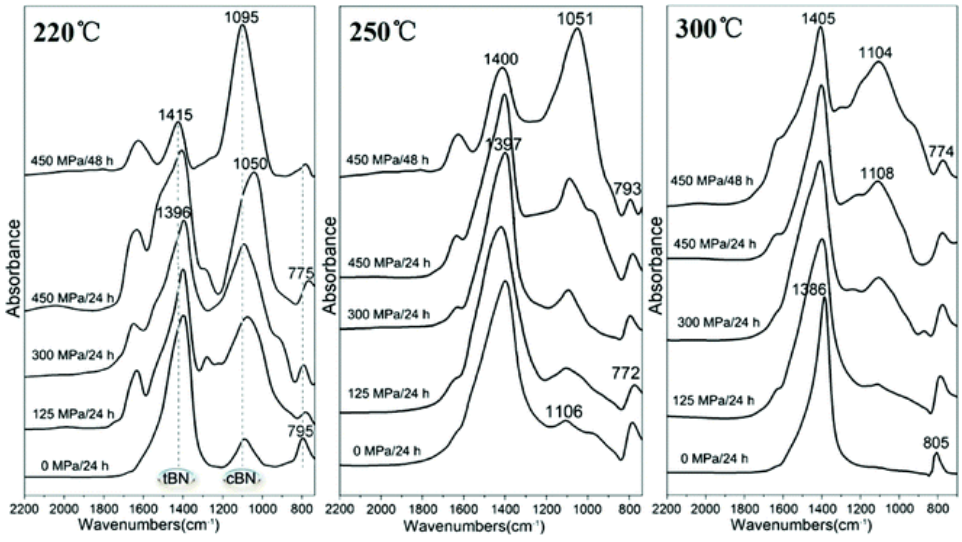

Figure 11: FTIR spectra of BN samples.

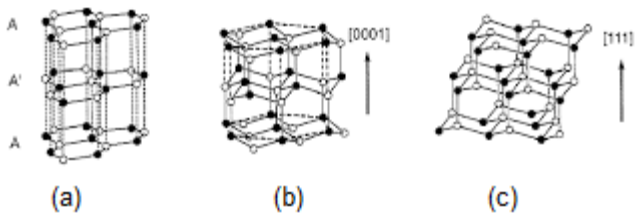

Figure 12: Structure of (a) h-BN, (b) w-BN and (c) c-BN.

4. CONCLUSION

The shear stress is high at the interface resulting to interphase debonding in AA8090/ BN composites. The particle fracture was observed above room temperature loading in AA8090/BN composites. The debonding was noticed above 100°C of thermal loading. The microstructure obtained from the experimental samples confirms the fracture of interphase between the BN particles and AA8090 alloy matrix and particle fracture. The BN nanoparticle fracture may be attributed to phase transformation.

REFERENCES

1. A. C. Reddy, Mechanical properties and fracture behavior of 6061/SiCp Metal Matrix Composites Fabricated by Low Pressure Die Casting Process, Journal of Manufacturing Technology Research, 1, 2009, pp.273-286.
2. A. C. Reddy, Tensile properties and fracture behavior of 6063/SiC_P metal matrix composites fabricated by investment casting process, International Journal of Mechanical Engineering and Materials Sciences, 3, 2010, pp.73-78.
3. A. C.a Reddy and B. Kotiveerachari, Effect of aging condition on structure and the properties of Al-alloy / SiC composite, International Journal of Engineering and Technology, 2, 2010, pp.462-465.
4. A. C. Reddy and B. Kotiveerachari, Influence of microstructural changes caused by ageing on wear behaviour of Al6061/SiC composites, Journal of Metallurgy & Materials Science, 53, 2011, pp. 31-39.
5. A. C. Reddy, Tensile fracture behavior of 7072/SiCp metal matrix composites fabricated by gravity die casting process, Materials Technology: Advanced Performance Materials, 26, 2011, pp. 257-262.
6. A. C. Reddy, Influence of strain rate and temperature on superplastic behavior of sinter forged Al6061/SiC metal matrix composites, International Journal of Engineering Research & Technology, 4, 2011, pp.189-198.
7. A. C. Reddy , Evaluation of mechanical behavior of Al-alloy/SiC metal matrix composites with respect to their constituents using Taguchi techniques, i-manager's Journal of Mechanical Engineering, 1, 2011, pp.31-41.
8. A. C. Reddy and Essa Zitoun, Matrix al-alloys for alumina particle reinforced metal matrix composites, Indian Foundry Journal, 55, 2009, pp.12-16.
9. A. C. Reddy and Essa Zitoun, Tensile behavior of 6063/Al_2O_3 particulate metal matrix composites fabricated by investment casting process, International Journal of Applied Engineering Research, 1, 2010, pp.542-552.
10. A. C. Reddy and Essa Zitoun, Tensile properties and fracture behavior of 6061/Al_2O_3 metal matrix composites fabricated by low pressure die casting process, International Journal of Materials Sciences, 6, 2011, pp.147-157.
11. A. C. Reddy, Strengthening mechanisms and fracture behavior of 7072Al/Al_2O_3 metal matrix composites, International Journal of Engineering Science and Technology, 3, 2011, pp.6090-6100.
12. A. C. Reddy, Evaluation of mechanical behavior of Al-alloy/Al_2O_3 metal matrix composites with respect to their constituents using Taguchi, International Journal of Emerging Technologies and Applications in Engineering Technology and Sciences, 4, 2011, pp. 26-30.
13. A. C. Reddy, Stir Casting Process on Porosity Development and Micromechanical Properties of AA5050/Titanium Oxide Metal Matrix Composites, 5th National Conference on Materials and Manufacturing Processes, Hyderabad, 9-10 June 2006, pp. 144-148.
14. A. C. Reddy, Sliding Wear and Micromechanical Behavior of AA1100/Titanium Oxide Metal Matrix Composites Cast by Bottom-Up Pouring, 7th International Conference on Composite Materials and Characterization, Bangalore, 11-12 December 2009, 205-210.
15. A. C.a Reddy, Effect of Clustering Induced Porosity on Micromechanical Properties of AA6061/Titanium Oxide Particulate Metal matrix Composites, 6th International Conference on Composite Materials and Characterization, Hyderabad, 8-9 June 2007, pp. 149-154.
16. P. Rami Reddy, A. C. Reddy, Processing of AA4015-Zirconium Oxide Particulate Metal Matrix Composites by Stir Casting Technology, 7th International Conference on Composite Materials and Characterization, Bangalore, 11-12 December 2009, 221-224.
17. A. C. Reddy, Effect of Porosity Formation during Synthesis of Cast AA4015/Titanium Nitride Particle-Metal Matrix Composites, 5th National Conference on Materials and Manufacturing Processes, Hyderabad, 9-10 June 2006, pp. 139-143.
18. A. C. Reddy, Role of Porosity and Clustering on Performance of AA1100/Boron Carbide Particle-Reinforced Metal Matrix Composites, 6th International Conference on Composite Materials and Characterization, Hyderabad, 8-9 June 2007, pp. 122-127.
19. S. Pitchi Reddy, A. C. Reddy, Synthesis and Characterization of Zirconium Carbide Nanoparticles Reinforced AA2024 Alloy Matrix Composites Cast by Bottom-Up Pouring, 7th International Conference on Composite Materials and Characterization, Bangalore, 11-12 December 2009, 211-215.
20. A. C. Reddy, Studies on fracture behavior of brittle matrix and alumina trihydrate particulate composites, Indian Journal of Engineering & Materials Sciences, 9, 2003, pp.365-368.
21. A. C. Reddy, Wear and Mechanical Behavior of Bottom-Up Poured AA4015/Graphite Particle-Reinforced Metal Matrix Composites, 6th National Conference on Materials and Manufacturing Processes, Hyderabad, 8-9 August 2008, pp. 120-126.

22. Essa Zitoun, A. C. Reddy, Analysis of Micromechanical Behavior of AA3003 Alloy - Graphite Metal Matrix Composites Cast by Bottom-Up Pouring with Regard to Agglomeration and Porosity, 7th International Conference on Composite Materials and Characterization, Bangalore, 11-12 December 2009, 216-220.
23. A. A. Shulzhenko (Ed.), Sintez, Spekaniye i Svoystva Sverkhtverdykh Materialov (Treatises), Institute for Superhard Materials, Kiev, 2000, pp. 131144.
24. A.V. Kurdyumov, V.F. Britun, and I.A. Petrusha, Structural mechanisms of rhombohedral BN transformations into diamond-like- phase, Diamond Related Materials, 5, 1996, p.1229.
25. J. Furthm¨uller, J. Hafner, and G. Kresse, Structural and Electronic Properties of Clean and Hydrogenated Diamond (100) Surfaces, Physical Review Letter, B 50, 1994, 15606.
26. L. Vel, G. Demazeau, and J. Etourneau, Cubic born nitride: synthesis, physicochemical properties and applications, Materials Science and Engineering B 10, 1991, pp. 149-164.